

Modification of sugarcane bagasse as polymer composite reinforcement via alkalization and benzylolation

Sulaiman Thalib^{1*}, Sarani Zakaria², Che Husna Azhari³,
Ikramullah Muhammad¹, and Husni Usman¹

¹Department of Mechanical and Industrial Engineering, University of Syiah Kuala, Banda Aceh 23111, Indonesia

²Department of Mechanical Engineering Technology, University of Malaysia Perlis, Arau 02600, Malaysia

³Department of Mechanical and Manufacturing Engineering, The National University of Malaysia, Bangi, Malaysia

*Corresponding Author: sulaimanthalib@usk.ac.id

Abstract

This research evaluates the impact of chemical modification on the thermal, structural, chemical, and mechanical properties of sugarcane bagasse particles for their application as reinforcement in polymer composites, which was conducted through alkalization and subsequent benzylolation. Sugarcane bagasse was first mechanically refined, then treated with sodium hydroxide to produce alkalized bagasse (ALC), followed by etherification with benzyl chloride to yield benzylated bagasse (BLC). The untreated and modified particles were characterized using TGA, DSC, XRD, FTIR, and tensile testing. Thermal analysis showed degradation temperatures of 250 °C, 245 °C, and 240 °C for untreated, ALC, and BLC, respectively. XRD revealed a decrease in crystallinity after treatment, indicating increased amorphous content due to surface modification. FTIR confirmed the replacement of hydroxyl groups with benzyl groups, enhancing hydrophobicity. Mechanical testing demonstrated a significant improvement in the tensile strength and modulus of PA6 composites reinforced with BLC, with the highest values (49.5 MPa and 1224.3 MPa) achieved using 100 µm BLC particles. These results highlight the effectiveness of chemical modification in improving interfacial compatibility and mechanical performance, supporting the use of modified bagasse as a sustainable reinforcement for bio-based composites.

Keywords:

Bagasse particle, thermal properties, X-ray diffraction, FTIR

1 Introduction

There is an increasing use of natural fibers (*lignocellulosic*) from agricultural resources like straw, jute, sisal, bagasse, knaf and other natural fibers as filler or reinforcement matrices of thermoplastic composites or thermoset composites [1]. The advantages of natural fibers are low density, high specific strength, low cost and availability of renewable resources, non-toxic, and degradable in the environment [2,3]. The disadvantages of natural fibers are hydrophilicity properties, these properties cause poor wettability and absorbability toward polymers; however, the adhesion between the fibers and polymer matrices is generally insufficient. To improve the interfacial bonding, surface modification of the fibres or plasticization of the fibres [4].

The sugarcane bagasse is a waste of agricultural resources or a waste of the sugarcane industry. A Fibrous residue of cane stalks is left over after the crushing and extraction of juice from the sugarcane. It is a lignocellulosic by-product of the sugar and alcohol

industries. The bagasse is used as fuel by sugarcane factories [5]. The sugarcane bagasse is a lignocellulosic material consisting of cellulose, hemicellulose, and lignin. Lignin and hemicelluloses possess thermoplastic properties. Cellulose is a thermoset, leaner polymer having the glucose residue as a repeating unit [6]. The molecule of glucose has three hydroxyl groups and tends to form hydrogen bonds. Cellulose has a high degree of crystallinity [7]. The crystalline structure of cellulose can be changed by substitution of it's with a suitable chemical reagent. This process decreased of crystallinity degree of cellulose and improved the thermoplastic properties of cellulose. The substitution groups act as plasticizers. The chemical modifications of natural fibers affect to pyrolysis properties of lignocellulose [8].

In this study, sugarcane bagasse fibers were chemically modified through alkaline treatment and benzylolation to enhance their material properties. These modifications were intended to improve the compatibility of the fibers with polymer matrices. Thermogravimetric Analysis (TGA) and Differential Scanning Calorimetry (DSC) were used to investigate thermal behavior, while X-Ray Diffraction (XRD) was employed to analyze crystallinity and crystallite size. Fourier Transform Infrared (FTIR) spectroscopy was used to examine changes in chemical structure, and Energy-Dispersive X-ray (EDX) spectroscopy was used to assess the elemental composition of the samples. Mechanical testing was carried out to evaluate the tensile performance of PA6 composites reinforced with the treated bagasse particles. The objective of this research is to evaluate how chemical modification through alkalization and benzylolation affects the thermal, structural, chemical, and mechanical properties of sugarcane bagasse, to improve its performance as a natural fiber reinforcement in polymer composites.

2 Materials and methods

The sugarcane bagasse from the wastes of the sugarcane industry was used in this investigation. The bagasse was washed to remove sugar residue and then dried. The powders of sugarcane bagasse were prepared by using Refining Mechanical Pulp (RMP). The powder of sugarcane bagasse was subjected to chemical modifications with alkalized and benzylolation to improve compatibility between the thermoplastic matrices and sugarcane bagasse particles.

Chemical modification was conducted by dipping in 10% aqueous sodium hydroxide as a fiber-swelling agent for a long 30 minutes, after which the solid was recovered by filtration. The benzylated process was conducted on alkaline-pretreated bagasse powder. The alkaline-pretreated bagasse powder was placed in a reaction flask with 125 ml of benzyl chloride. The mixture was allowed to react for 2 hours at 100 °C. The reacted sugarcane bagasse powder was then soaked in a water: methanol (1:1 v/v) mixture for 24 hours. The methanol was removed by filtration, and the solid was washed under flowing tap water. Two kinds of samples were prepared for this investigation, that was alkalized and benzylated sugarcane bagasse powder. The reacted powders were air-dried for 24 hours, followed by drying in the dryer at 70 °C for 24 hours.

Samples prepared for thermal analysis, XRD in powder form, and samples for FTIR were prepared from bagasse particles with KBr and shaped into pellet form. The samples for Edax analysis were prepared from bagasse particles with gold coating. The thermal behaviour of bagasse particles was studied by Thermogravimetry (TG) and DSC. The specimens were scanned from 25 – 600 °C at a heating rate of 10 °C/min in the present nitrogen. The equipment includes a Mettler, Toledo DSC (DEMO version) and a Mettler, Toledo TGA (TGA 851E). XRD analysis was conducted using an X-ray diffractometer (D5000-Siemens). The diffraction intensity was measured at angles (2θ) ranging from 5° to 55°, with a step size of 0.04°. The analysis utilized monochromatic CuKα radiation, which has a wavelength of 0.154 nm. The collected data was plotted to display XRD intensity as a function of the scattering angle (2θ). This method, which employs powder diffraction or analytical techniques,

provides comprehensive information about the samples [9]. The FTIR spectrometry Shimadzu 8210 PC was conducted to studied chemical structure of samples. Sugarcane bagasse particles were mixed with KBr and were shaped in pellet form. The data was collected in range spectrum start from 500 cm^{-1} to 4000 cm^{-1} [10]. Analysis chemical compositions of samples were conducted EDAX spectroscopy, it's attached of SEM equipment. The sample of sugarcane bagasse powder was coated with gold.

The composite manufacturing process was carried out through melt compounding using a twin-screw extrusion technique. Initially, dried bagasse particles were continuously mixed with polyamide 6 (PA6) granules, forming a dry blend that advanced linearly toward the extruder inlet. Pre-mixing was conducted prior to feeding, and the dry mixture was simultaneously introduced into the extruder hopper. Throughout the extrusion process, precise control of operational parameters was maintained to ensure uniform dispersion and the production of high-quality composite materials. The extrusion relied on radial mixing induced by the extruder screw. Compared to single-screw extruders, twin-screw extruders provide enhanced radial and distributive mixing capabilities [11]. Therefore, a co-rotating twin-screw extruder (Brabender DSK 42/7) was employed, equipped with screws of 41.8 mm diameter and 328 mm length, yielding a length-to-diameter (L/D) ratio of 7.

Processing parameters were set as follows: screw rotation speed of 40 rpm, and barrel temperatures of $210\text{ }^{\circ}\text{C}$, $220\text{ }^{\circ}\text{C}$, and $220\text{ }^{\circ}\text{C}$ across the heating zones. These values fall within the melting range of PA6. However, due to internal shear and frictional heating during processing, the actual temperature within the barrel rose to approximately $230\text{ }^{\circ}\text{C}$, about $10\text{ }^{\circ}\text{C}$ above the PA6 melting point. Shear forces developed both among PA6 chains and between bagasse particles, while friction occurred between the bagasse particles and the molten polymer, the barrel wall, and the rotating screws. Temperature control within the melting range of PA6 was critical to prevent thermal degradation or carbonization of the bagasse particles, which would otherwise lead to undesirable discoloration and compromised composite quality.

To enhance interfacial adhesion and compatibility with the PA6 matrix, bagasse fibers were subjected to surface treatment using a 12.5% sodium hydroxide (NaOH) solution followed by benzyl chloride treatment. The treated fibers were then sieved to obtain particle sizes of $40\text{ }\mu\text{m}$, $63\text{ }\mu\text{m}$, and $100\text{ }\mu\text{m}$, which were subsequently used as reinforcement in the composite formulation. The extrusion process yielded continuous strands of PA6/bagasse composites with an approximate diameter of 5 mm. Upon exiting the die, these strands underwent phase transition from the molten to the solid state and were cooled in ambient air. The resulting strands exhibited color variations ranging from light to dark brown, depending on the relative content of bagasse particles. Higher concentrations of bagasse resulted in darker composite strands. The extruded strands were finally pelletized into uniform composite granules for further processing. Subsequently, tensile testing was conducted on the composite samples to evaluate their mechanical performance, specifically the maximum tensile strength and elastic modulus. The tests were performed in accordance with the ASTM D638 standard using an INSTRON® Universal Testing Machine.

3 Results and discussion.

3.1 Thermal properties

This investigation conducted a thermal analysis with TG and DSC. The specimens were scanned and resulted in TG and DSC of alkalized sugarcane bagasse and benzylated sugarcane bagasse samples as followed.

3.1.1 TGA

Thermogravimetric analyses of samples (pure bagasse, Alkalized Bagasse (ALC), and BLC) were plotted in graphs showing weight loss versus temperature. The plotted results are presented in Figs. Fig. 1, Fig. 2, and Fig. 3. The graphs indicate three temperature regions. For pure bagasse, the temperature ranges are $45\text{ }^{\circ}\text{C}$ - $80\text{ }^{\circ}\text{C}$,

$250\text{ }^{\circ}\text{C}$ - $430\text{ }^{\circ}\text{C}$, and above $430\text{ }^{\circ}\text{C}$. For ALC, the ranges are $45\text{ }^{\circ}\text{C}$ - $80\text{ }^{\circ}\text{C}$, $245\text{ }^{\circ}\text{C}$ - $415\text{ }^{\circ}\text{C}$, and above $415\text{ }^{\circ}\text{C}$. For BLC, the ranges are $25\text{ }^{\circ}\text{C}$ - $80\text{ }^{\circ}\text{C}$, $240\text{ }^{\circ}\text{C}$ - $430\text{ }^{\circ}\text{C}$, and above $430\text{ }^{\circ}\text{C}$. These temperature ranges were considered when discussing the thermal stability of bagasse particles.

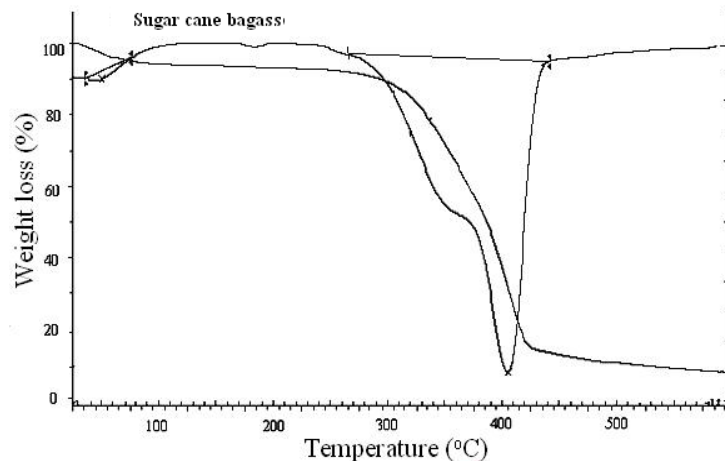


Fig. 1. TG and TGA thermograms of pure bagasse

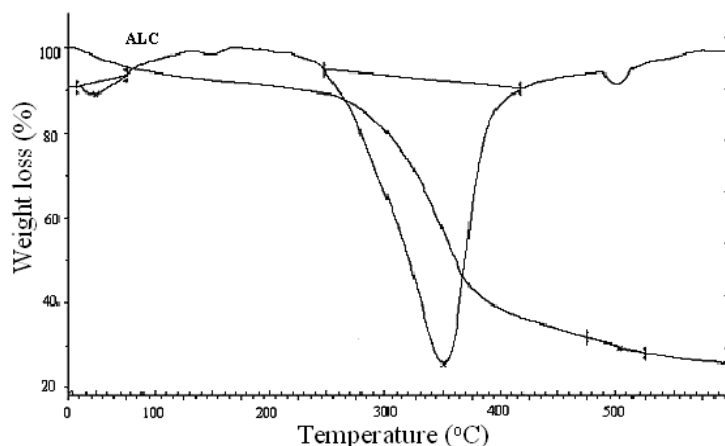


Fig. 2. TG and TGA thermograms of ALC

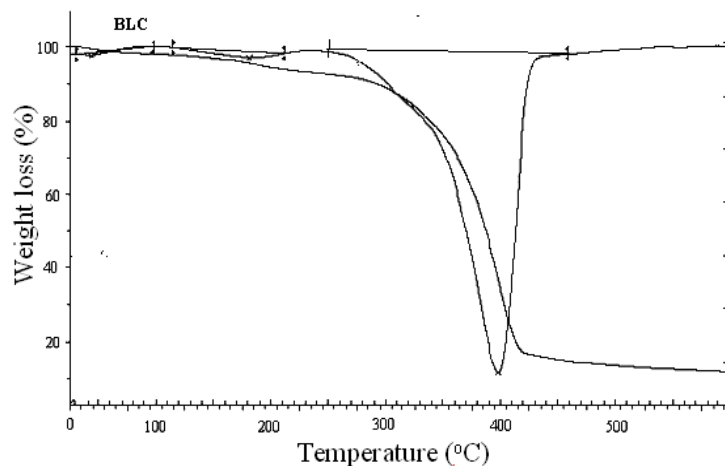


Fig. 3. TG and TGA thermograms of Benzylated Bagasse (BLC)

The particles exhibited good stability in the temperature range of $80\text{ }^{\circ}\text{C}$ to $250\text{ }^{\circ}\text{C}$ for pure bagasse, $80\text{ }^{\circ}\text{C}$ to $245\text{ }^{\circ}\text{C}$ for ALC, and $80\text{ }^{\circ}\text{C}$ to $240\text{ }^{\circ}\text{C}$ for BLC. In the first stage, pure bagasse and ALC experienced a weight loss of 5% in the temperature range of $45\text{ }^{\circ}\text{C}$ - $80\text{ }^{\circ}\text{C}$, while BLC experienced a weight loss of 2% in the range of $25\text{ }^{\circ}\text{C}$ - $80\text{ }^{\circ}\text{C}$. This weight loss was attributed to the vaporization of water, indicating that dehydration of the bagasse particles occurred. In the second stage, pure bagasse showed a weight loss of 75% in the temperature range of $250\text{ }^{\circ}\text{C}$ - $430\text{ }^{\circ}\text{C}$, ALC showed a weight loss of 55% in the range of $245\text{ }^{\circ}\text{C}$ - $415\text{ }^{\circ}\text{C}$, and BLC showed a weight loss of 75% in the range of $240\text{ }^{\circ}\text{C}$ - $430\text{ }^{\circ}\text{C}$. The weight loss in this stage was caused by the thermal depolymerization of hemicelluloses and the cleavage of glycosidic linkages in cellulose. The third stage

began at approximately 430 °C for pure bagasse, with a weight loss of 20%; at 415 °C for ALC, with a weight loss of 10%; and at 430 °C for BLC, with a weight loss of 5%. The weight loss in this stage was due to the further breakdown of the decomposition products from the second stage, leading to tar formation through levoglucosan [12,13].

The TGA thermograms of pure bagasse, ALC, and BLC are shown in Figs. Fig. 1, Fig. 2, and Fig. 3. The pure bagasse particles have a small peak at 52 °C and a big peak at 405 °C. The small peak showed the vaporization process of water of the samples and the big peaks showed depolymerisation of hemicelluloses of the samples. The ALC sample has three peaks, the first peak at 52 °C showed the vaporization process of water of samples, the second peak as a big peak at 350 °C, showed depolymerisation of hemicelluloses of samples, and the third peak at 500 °C was further breakage of the decomposition product before. The BLC sample have a peak at 400 °C, this peak showed the depolymerisation of hemicelluloses of the sample. Thermal stability of sugarcane bagasse particles as filler of composite are important matter to consider in the composite process. The thermal analysis showed sugarcane bagasse particles are suitable as filler of composite and stable up to temperature blends at 250 °C of pure bagasse and 245 °C of ALC and 240 °C of BLC. The thermal stability of natural fibres with modifications was reported [12–15].

3.1.2 DSC

The decomposition of pure sugarcane bagasse particles, as well as chemically modified versions (ALC and BLC), was analyzed using DSC. The thermograms, illustrated in Fig. 4, reveal a consistent trend across all samples.

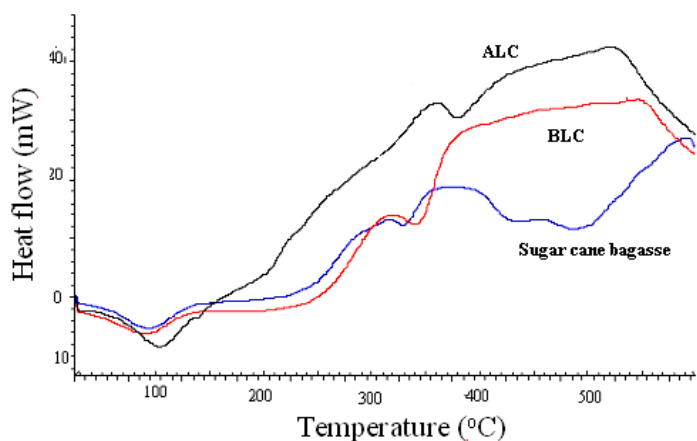


Fig. 4. DSC Thermogram of sugar cane bagasse, ALC and BLC

The DSC thermogram indicates endothermic peaks within the temperature range of 30 °C to 150 °C, with specific peak temperatures of 120 °C for pure bagasse, 95 °C for ALC, and 100 °C for BLC. These endothermic events are likely attributed to the natural lattice structures present in the bagasse and the evaporation of moisture. Notably, pure bagasse exhibits a broader evaporation range compared to the chemically modified bagasse particles, suggesting a higher moisture content in the pure sample.

Additionally, the thermogram displays two exothermic peaks for each sample. For pure bagasse, these peaks occur in the ranges of 250 °C to 325 °C and 330 °C to 445 °C. For ALC, the exothermic peaks are found between 245 °C and 375 °C, and 380 °C to 485 °C. BLC shows exothermic peaks at 240 °C to 340 °C and 345 °C to 465 °C. The first exothermic peak is indicative of the decomposition of bagasse particles, while the second peak reflects a reduction in crystallinity, which is essential for assessing the thermal degradation of crystallites within the bagasse [16].

Interestingly, pure bagasse also exhibits a fourth exothermic peak, which is interpreted as the combustion of the bagasse particles. This comprehensive analysis of the thermal behavior of sugarcane bagasse and its modifications provides valuable insights into their thermal stability and degradation characteristics

The results of the DSC analysis indicate that the processing of bagasse particles can be effectively conducted at specific maximum temperatures to ensure safety and efficiency. It is crucial to process bagasse particles below their maximum processing temperatures to mitigate the risk of fire [17].

The maximum processing temperatures identified for the different types of bagasse particles are as follows: pure bagasse at 250 °C, ALC (alkaline-treated bagasse) at approximately 245 °C, and BLC at around 240 °C. When considering the use of bagasse particles as reinforcement in thermoplastic composites, polyamide 6 (PA6) is a suitable matrix material. The processing temperature for polyamide 6 is around 220 °C, which is below the maximum processing temperatures of the bagasse particles.

3.2 The crystallinity properties of sugarcane bagasse

The crystallinity properties of sugarcane bagasse were studied using the XRD technique. The technique can be used to estimate the crystallinity and mean crystallite size of cellulose in samples. The crystallinity in materials is practically and easily known qualitatively exactly using X-ray diffraction.

The X-ray diffractogram of cotton as a reference is shown in Fig. 5. The cellulose content of cotton is 100%. The crystallinity analysis of cotton showed of hkl plane (022) were on 2θ at 22.6° . (101) at 14.6° and (101) at 6.2° . The plane of cotton was 100% Cellulose I. Crystallinity of pure bagasse, ALC, and BLC was shown in XRD spectrum Figs. Fig. 6, Fig. 7, and Fig. 8 respectively. From the XRD spectrum of pure bagasse, ALC and BLC can be found $I_{(002)}$, I_{lam} , RCr , D_{hkl} and I_c . are showed in Table 1.

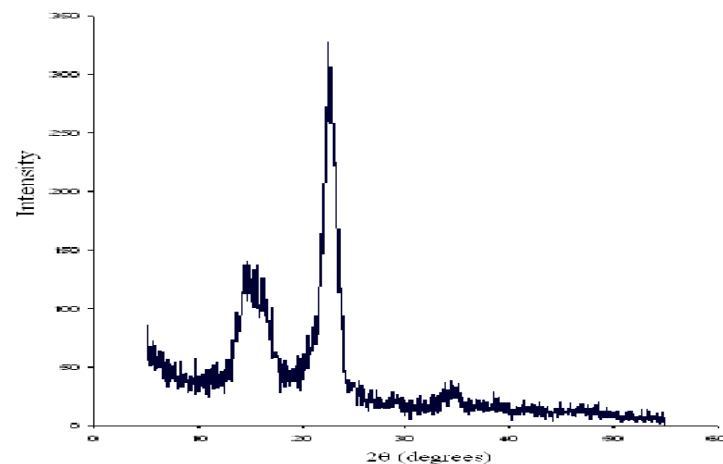


Fig. 5. XRD spectra of cotton as reference

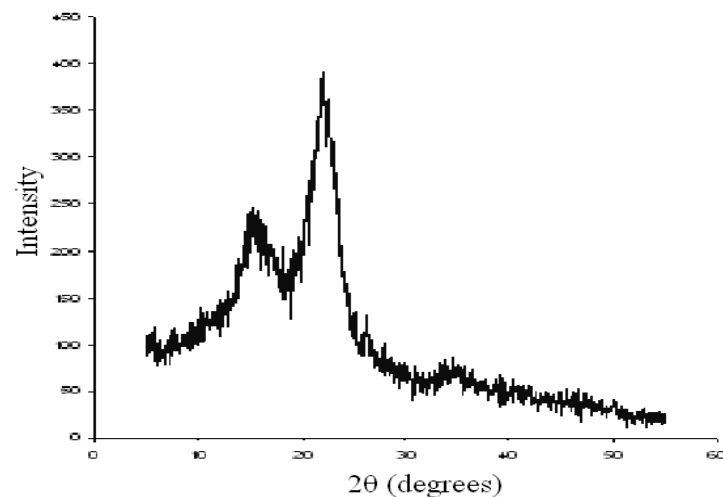


Fig. 6. XRD spectra of pure bagasse

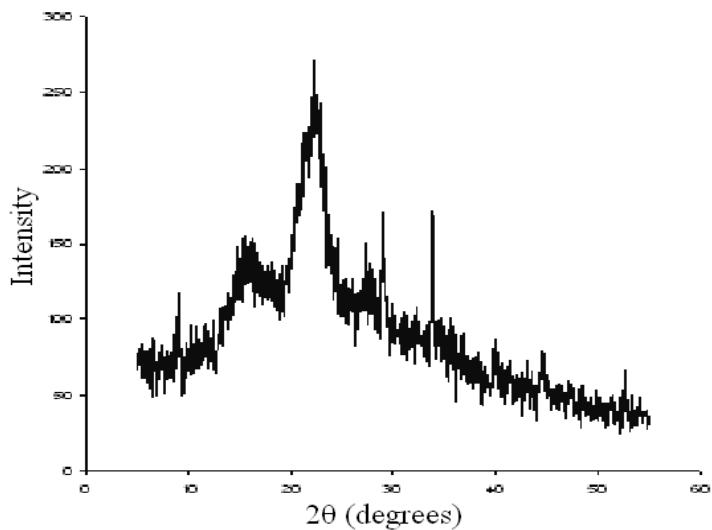


Fig. 7. XRD spectra of ALC

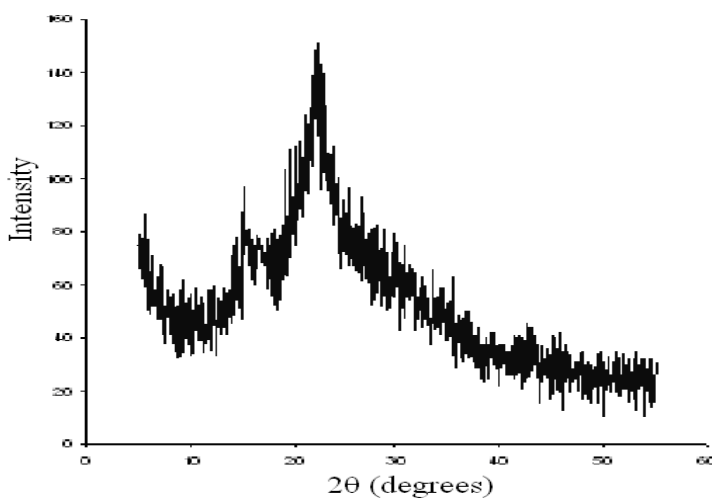


Fig. 8. XRD spectra of BLC

Table 1. XRD Intensity of crystallinity (002) plane, amorphous intensity, ratio of crystallinity, mean crystallinity dimension and Crystallinity Index of pure bagasse, ALC and BLC

Sample	$I_{(002)}$	I_{am}	$I_{cr(002)}$	RCr	2θ	Cos θ	$\beta_{1/2}$ (°)	D_{hkl} (nm)	I_c (%)
Pure Bagasse	391	78	313	1	22.07	0.9969	3.5	2.58	60.6
ALC	272	51	221	1.41	22.19	0.9803	4.15	1.93	54.8
BLC	151	34	267	2.67	22.14	0.9889	6.05	1.31	52

X-ray diffractograms of various bagasse particles exhibited similar spectral profiles to that of cotton, which served as a reference. The XRD analysis confirmed the presence of cellulose I in all samples. The characteristic peaks of the XRD spectra were observed at 22.07° for pure bagasse, 22.19° for ALC, and 22.14° for BLC. Notably, these peaks shifted to the left compared to the cotton peak, which was located at 22.6°. The chemical modifications applied to the bagasse samples resulted in slight shifts in the peak positions, with ALC showing a peak at 22.19° and BLC at 22.14°. These findings align with the XRD profiles of cellulose reported by [18].

The crystallinity indexes calculated for the samples were 60.6% for pure bagasse, 54.8% for ALC, and 52% for BLC. Additionally, the D002 values for ALC and BLC were found to be 1.31, which is 1.93 times smaller than the D002 value of pure bagasse. This reduction in crystallinity can be attributed to the chemical modifications, which led to a decrease in crystallinity during the chemical reactions. These reactions caused the interpolymer bonds between cellulose, hemicellulose, and lignin macromolecules within the particles to loosen [18].

The observed decrystallinity was reflected in the changes in peak positions within the X-ray diffractograms. The structure of bagasse consists of both crystalline and amorphous regions. The chemical modifications resulted in a decrease in the crystalline index, leading

to a relatively larger amorphous region compared to the crystalline region. Consequently, this alteration in structure resulted in a decrease in the thermal stability of the modified samples.

3.3 FTIR analysis

FTIR spectroscopy was employed to analyze the vibrational modes of chemical functional groups in the bagasse samples. When infrared radiation interacts with the samples, the chemical bonds undergo stretching, twisting, and contracting, which is reflected in the absorption of infrared radiation at specific wavenumbers. The FTIR spectrum covers a wavenumber range from 12,800 cm^{-1} to 10 cm^{-1} , corresponding to wavelengths from 0.78 μm to 1000 μm . The FTIR analyses of pure bagasse, ALC, and BLC are presented in Fig. 9, with the infrared absorption data summarized in Table 2.

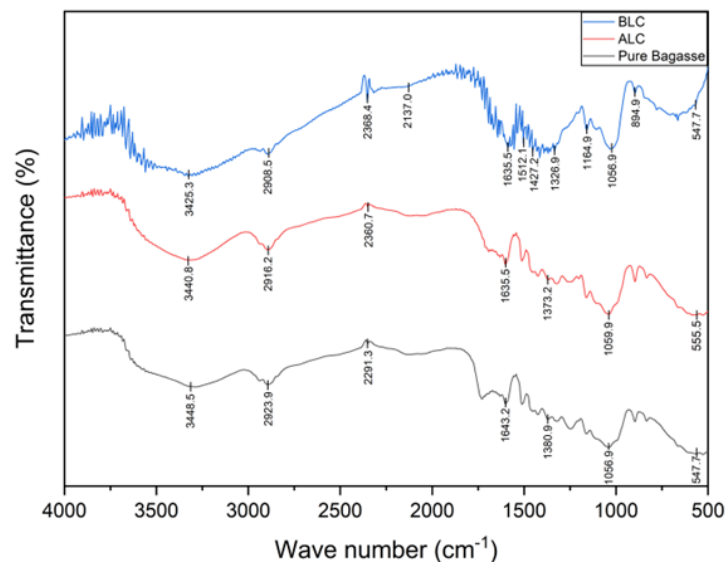


Fig. 9. FTIR spectra of pure bagasse, ALC, and BLC

Table 2. Infrared absorption of pure bagasse, ALC and BLC

Pure bagasse		ALC		BLC		Function group
Wave Number (cm^{-1})	Absorption	Wave Number (cm^{-1})	Absorption	Wave Number (cm^{-1})	Absorption	
3448.5	15.685	3440.8	11.106	3425.3	14.454	O-H (hydrogen bonding)
2923.9	45.497	2916.2	31.24	2908.5	51.547	C-H
2291.3	60.824	-	-	-	-	Phosphorus acid & ester P-H stretching
-	-	2360.7	43.131	2368.4	62.836	Phosphine P-H stretching
-	-	-	-	2137	65	C=C alkynes group stretching
1643.2	45.842	1635.5	29.399	1635.5	46.687	C=C alkenes group stretching
-	-	-	-	1512.1	57.343	C=C aromatic ring vibration
1380.9	52.31	1373.2	31.38	-	-	C-H
-	-	-	-	1427.2	53.425	C=C aromatic ring vibration
-	-	-	-	1326.9	52.383	C-N
-	-	-	-	1164.9	42.462	C-H
1056.9	48.66	1056.9	22.962	1056.9	31.001	C-H
-	-	-	-	894.9	57.91	C-H

The spectra reveal significant changes in the hydroxyl (O-H) groups, particularly in the intensity of hydrogen bonds. The stretching vibration of the O-H bond in pure bagasse appears at 3448.5 cm^{-1} , which shifts to 3440.8 cm^{-1} for ALC and further to 3425.3 cm^{-1} for BLC. This rightward shift indicates a decrease in hydrogen bonding intensity, with ALC showing an 11.106% increase in absorption. The shift to 3425.3 cm^{-1} in BLC suggests a

transformation of hydroxyl groups (O-H) into benzyl groups. The intensity of the peaks associated with C-H stretching vibrations is relatively low, with pure bagasse showing a peak at 2923.9 cm^{-1} , ALC at 2916.2 cm^{-1} , and BLC at 2908.5 cm^{-1} . These peaks indicate the presence of C-H_n bonds in aliphatic and aromatic structures across all samples [19].

Weak peaks corresponding to phosphorous acid and ester (P-H) stretching are observed at 2291.3 cm^{-1} for pure bagasse, while ALC and BLC show weak peaks at 2360.7 cm^{-1} and 2368.4 cm^{-1} , respectively. The shifting of these peaks indicates a transition from phosphorous acid and ester P-H stretching to phosphine P-H stretching, confirming the presence of phosphorus in all samples.

The stretching vibrations of C=C bonds are noted at 1643.2 cm^{-1} for pure bagasse and 1635.5 cm^{-1} for ALC, while BLC also shows a peak at 1635.5 cm^{-1} , indicating the presence of alkenes. Additionally, BLC exhibits a weak peak at 2137 cm^{-1} , associated with alkynes, and peaks at 1512.1 cm^{-1} and 1427.2 cm^{-1} , which correspond to C-C vibrations in aromatic rings. A peak at 1326.9 cm^{-1} is attributed to C-N stretching. Notably, these last four peaks are absent in pure bagasse and ALC, indicating that the hydroxyl groups in these samples have been replaced by aromatic rings due to benzylation. The chemical modifications led to the loss of hydroxyl groups in pure bagasse and ALC as a result of alkalization and benzylation reactions, resulting in BLC being more hydrophobic compared to pure bagasse particles.

The stretching vibration appeared of pure bagasse, ALC at 1380.9, 1373.2 respectively, this is indicating C-H in sample. The peaks of BLC at 1164.9 cm^{-1} , 1056.9 cm^{-1} and, 894.9 are C-H in BLC sample, which is changed benzene ring from benzyl group. The same indication was seen in others investigation [18,19].

The energy dispersive analysis X-ray (EDAX) spectroscopy showed chemical compositions change when chemical modifications of bagasse occur. Chemical compositions contain of pure bagasse are 67.2% C, 32.8% O, ALC are 65.28% C, 31.87% O and 02.85Na. Chemical contains of BLC are 64.85%C, 34.24%O, 0.033%Na and 0.029Cl. The Na contains is residual of NaOH washing treatment previously process, while Cl source of benzylation treatment. The influences of chemical treatment are chemical composition changed in bagasse. The change of chemical compositions caused of chemical reactions and any inclusions of other element when processing.

3.4 Tensile properties analysis

The mechanical performance of the PA6/bagasse composites was evaluated through tensile testing to determine the maximum tensile stress and elastic modulus. The tensile stress-strain curve is shown in Fig. 10 and summarized in Figs. Fig. 11 and Fig. 12, revealing the effects of fiber treatment and particle size on the tensile properties of the composites.

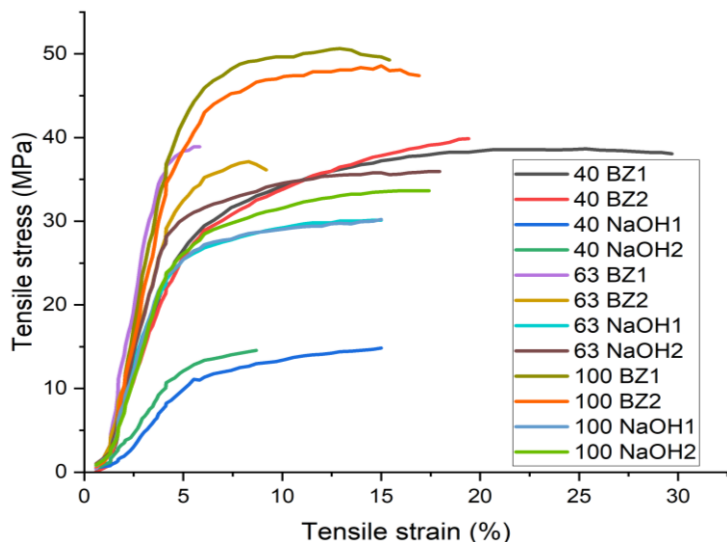


Fig. 10. Tensile stress-strain graph of PA6/bagasse composites

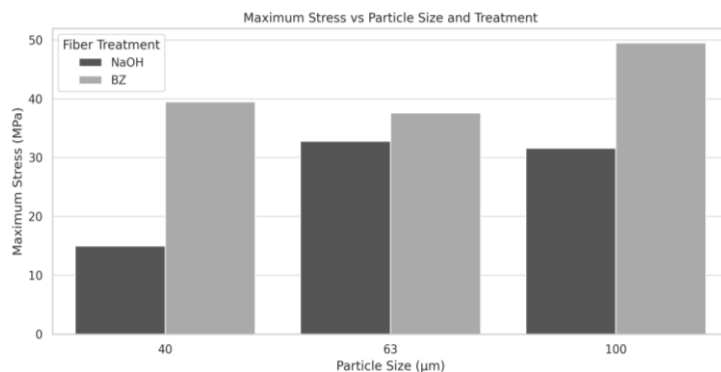


Fig. 11. Maximum tensile stress of PA6/bagasse composites as a function of particle size and fiber treatment

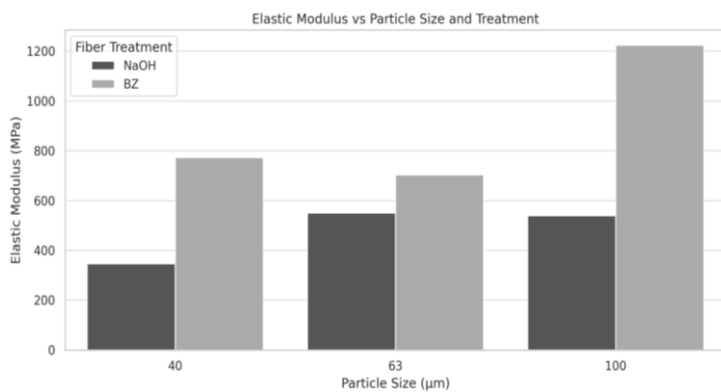


Fig. 12. Elastic modulus of PA6/bagasse composites as a function of particle size and fiber treatment

Fiber treatment played a critical role in enhancing mechanical performance. Composites reinforced with Benzyl Chloride (BZ)-treated bagasse fibers exhibited significantly higher tensile strength and stiffness compared to those treated with sodium hydroxide (NaOH) alone. For instance, at a particle size of 100 μm , BZ-treated fibers achieved the highest values of maximum stress (49.5 MPa) and elastic modulus (1224.3 MPa), representing an increase of over 50% and 125%, respectively, relative to their NaOH-treated counterparts. This improvement is attributed to enhanced interfacial bonding between the treated fibers and the PA6 matrix. The benzylation process likely reduced the hydrophilicity of the bagasse surface and improved compatibility with the hydrophobic polymer, facilitating better stress transfer.

Particle size also influenced composite properties. For NaOH-treated fibers, the maximum tensile strength increased from 15.0 MPa (40 μm) to 32.8 MPa (63 μm), then slightly decreased to 31.6 MPa at 100 μm . A similar trend was observed for elastic modulus. This suggests an optimal size range (around 63 μm) for untreated fibers, where sufficient surface area and aspect ratio balance reinforcement effectiveness. In contrast, composites with BZ-treated fibers showed continuous improvement in both tensile strength and stiffness with increasing particle size. This indicates that the improved interfacial compatibility due to benzylation allowed larger fibers (100 μm) to better reinforce the matrix without compromising dispersion or stress transfer.

These findings emphasize the importance of chemical surface modification and particle size optimization in designing high-performance natural fiber-reinforced thermoplastic composites. Benzyl chloride treatment, especially when used with coarser particles (100 μm), demonstrates great potential for enhancing both strength and stiffness in bio-composite applications.

4 Conclusions

This study demonstrated that chemical modification of sugarcane bagasse via alkalization and benzylation effectively enhances its properties as a reinforcement material in polymer composites. The modified particles exhibited improved compatibility with hydrophobic polymer matrices such as PA6, as evidenced by increased hydrophobicity and reduced crystallinity, which facilitates

better dispersion and interfacial bonding. Thermal analysis confirmed that both ALC and BLC particles retained stability within the processing range of PA6. FTIR analysis verified successful benzylolation through hydroxyl group substitution, while mechanical testing showed that BLC particles significantly improved composite tensile strength and stiffness, particularly at a 100 µm particle size. These findings confirm that surface treatment and particle size optimization are critical to improving the mechanical performance of natural fiber-reinforced composites. Overall, benzylated sugarcane bagasse offers promising potential as a sustainable and high-performance reinforcement for eco-friendly polymer materials.

References

- [1] Akram Tamlicha, S. Rizal, I. Hasanuddin, M.M. Noor, I. Ikramullah, N. Nazaruddin, The Simulation Of Drop-Weight Impact Test On Ramie-Eglass Hybrid Fiber Composite For Jaloe Kayoh Wall Material, *Jurnal Polimesin* 22 (2024) 75–82. <https://doi.org/10.30811/JPL.V22I1.4645>.
- [2] A. Karimah, M.R. Ridho, S.S. Munawar, D.S. Adi, Ismadi, R. Damayanti, B. Subiyanto, W. Fatriasari, A. Fudholi, A review on natural fibers for development of eco-friendly bio-composite: characteristics, and utilizations, *Journal of Materials Research and Technology* 13 (2021) 2442–2458. <https://doi.org/10.1016/j.jmrt.2021.06.014>.
- [3] S. Syaubari, J. Dawood, M. Zaki, D. Bachtiar, Fabrication and characterization of antioxidant biodegradable plastic from mangrove starch, chitosan, and clove essential oil, *Jurnal Polimesin* 23 (2025) 134–141. <https://doi.org/10.30811/JPL.V23I2.6394>.
- [4] M.M. Hassan, M.H. Wagner, Surface Modification of Natural Fibers for Reinforced Polymer Composites: A Critical Review, *Reviews of Adhesion and Adhesives* 4 (2016) 1–46. <https://doi.org/10.7569/RAA.2016.097302>.
- [5] E.O. Ajala, J.O. Ighalo, M.A. Ajala, A.G. Adeniyi, A.M. Ayanshola, Sugarcane bagasse: a biomass sufficiently applied for improving global energy, environment and economic sustainability, *Bioresour Bioprocess* 8 (2021) 87. <https://doi.org/10.1186/s40643-021-00440-z>.
- [6] P.S. Sejati, F. Obounou Akong, F. Fradet, P. Gérardin, Understanding the thermoplasticization mechanism of wood via esterification with fatty acids: A comparative study of the reactivity of cellulose, hemicelluloses and lignin, *Carbohydr Polym* 324 (2024) 121542. <https://doi.org/10.1016/j.carbpol.2023.121542>.
- [7] K.S. Salem, N.K. Kasera, Md.A. Rahman, H. Jameel, Y. Habibi, S.J. Eichhorn, A.D. French, L. Pal, L.A. Lucia, Comparison and assessment of methods for cellulose crystallinity determination, *Chem Soc Rev* 52 (2023) 6417–6446. <https://doi.org/10.1039/D2CS00569G>.
- [8] B. Tsegaye, A. Ström, M.S. Hedenqvist, Thermoplastic lignocellulose materials: A review on recent advancement and utilities, *Carbohydrate Polymer Technologies and Applications* 5 (2023) 100319. <https://doi.org/10.1016/j.carpta.2023.100319>.
- [9] H. Khan, A.S. Yerramilli, A. D'Oliveira, T.L. Alford, D.C. Boffito, G.S. Patience, Experimental methods in chemical engineering: X-ray diffraction spectroscopy-XRD, *Can J Chem Eng* 98 (2020) 1255–1266. <https://doi.org/10.1002/cjce.23747>.
- [10] S.A. Khan, S.B. Khan, L.U. Khan, A. Farooq, K. Akhtar, A.M. Asiri, Fourier Transform Infrared Spectroscopy: Fundamentals and Application in Functional Groups and Nanomaterials Characterization, in: *Handbook of Materials Characterization*, Springer International Publishing, Cham, 2018: pp. 317–344. https://doi.org/10.1007/978-3-319-92955-2_9.
- [11] T.B. Arthur, N. Rahmanian, Process Simulation of Twin-Screw Granulation: A Review, *Pharmaceutics* 2024, Vol. 16, Page 706 16 (2024) 706. <https://doi.org/10.3390/PHARMACEUTICS16060706>.
- [12] A.P.S. Soares, J.S. de Freitas, M.G. Mothé, C.G. Mothé, Thermal evaluation of composites from coffee capsules residue with sugarcane bagasse by TG/DTA and DMA, *J Therm Anal Calorim* 142 (2020) 651–660. <https://doi.org/10.1007/s10973-020-10012-6>.
- [13] S. Saeed, M. Saleem, A. Durrani, Thermal performance analysis of sugarcane bagasse pretreated by ionic liquids, *J Mol Liq* 312 (2020) 113424. <https://doi.org/10.1016/j.molliq.2020.113424>.
- [14] M. Asim, M.T. Paridah, M. Chandrasekar, R.M. Shahroze, M. Jawaid, M. Nasir, R. Siakeng, Thermal stability of natural fibers and their polymer composites, *Iranian Polymer Journal* 29 (2020) 625–648. <https://doi.org/10.1007/s13726-020-00824-6>.
- [15] N.M. Nurazzi, M.R.M. Asyraf, M. Rayung, M.N.F. Norrrahim, S.S. Shazleen, M.S.A. Rani, A.R. Shafi, H.A. Aisyah, M.H.M. Radzi, F.A. Sabaruddin, R.A. Ilyas, E.S. Zainudin, K. Abdan, Thermogravimetric analysis properties of cellulosic natural fiber polymer composites: A review on influence of chemical treatments, *Polymers (Basel)* 13 (2021). <https://doi.org/10.3390/polym13162710>.
- [16] E.R. Zanatta, T.O. Reinehr, J.A. Awadallak, S.J. Kleinübing, J.B.O. dos Santos, R.A. Bariccatti, P.A. Arroyo, E.A. da Silva, Kinetic studies of thermal decomposition of sugarcane bagasse and cassava bagasse, *J Therm Anal Calorim* 125 (2016) 437–445. <https://doi.org/10.1007/s10973-016-5378-x>.
- [17] C. Leyva-Porras, P. Cruz-Alcantar, V. Espinosa-Solís, E. Martínez-Guerra, C.I. Piñón-Balderrama, I. Compean Martínez, M.Z. Saavedra-Leos, Application of Differential Scanning Calorimetry (DSC) and Modulated Differential Scanning Calorimetry (MDSC) in Food and Drug Industries, *Polymers (Basel)* 12 (2019) 5. <https://doi.org/10.3390/polym12010005>.
- [18] E. Sun, F. Sun, Z. Zhang, Y. Dong, Interface morphology and thermoplasticization behavior of bamboo fibers benzylated with benzyl chloride, *Surface and Interface Analysis* 48 (2016) 64–72. <https://doi.org/10.1002/sia.5889>.
- [19] N.K. Waghmare, S. Khan, Extraction and Characterization of Nano-cellulose Fibrils from Indian Sugarcane Bagasse- an Agro Waste, *Journal of Natural Fibers* 19 (2022) 6230–6238. <https://doi.org/10.1080/15440478.2021.1907831>.